Geophysical Research Letters

RESEARCH LETTER
10.1029/2019GL083264

Southern Hemisphere Atmospheric Blocking in CMIP5 and Future Changes in the Australia-New Zealand Sector

Matthew Patterson[1,2], **Thomas Bracegirdle**[2], **and Tim Woollings**[1]

[1]Atmospheric, Oceanic and Planetary Physics, University of Oxford, Oxford, UK, [2]British Antarctic Survey, Cambridge, UK

Key Points:
- We provide a comprehensive survey of Southern Hemisphere blocking using a large number of coupled models
- Future projections generally suggest an overall decrease in Southern Hemisphere blocking frequency
- There is strong model agreement on blocking frequency decreases to the south of Australia during austral winter

Supporting Information:
- Supporting Information S1
- Figure S1
- Figure S2
- Figure S3
- Figure S4
- Figure S5
- Figure S6
- Figure S7

Correspondence to:
M. Patterson,
matthew.patterson@physics.ox.ac.uk

Citation:
Patterson, M., Bracegirdle, T., & Woollings, T. (2019). Southern Hemisphere atmospheric blocking in CMIP5 and future changes in the Australia-New Zealand sector. *Geophysical Research Letters*, *46*, 9281–9290. https://doi.org/10.1029/2019GL083264

Received 12 APR 2019
Accepted 30 JUL 2019
Accepted article online 5 AUG 2019
Published online 13 AUG 2019

Abstract Many general circulation models fail to capture the observed frequency of atmospheric blocking events in the Northern Hemisphere; however, few studies have examined models in the Southern Hemisphere and those studies that have, have often been based on only a few models. To provide a comprehensive view of how the current generation of coupled general circulation models performs in the Southern Hemisphere and how blocking frequency changes under enhanced greenhouse gas forcing, we examine the output of 23 models from the Coupled Model Intercomparison Project Phase 5 (CMIP5). We find that models have differing biases during winter, when blocking occurrence is highest, though models underestimate blocking frequency south of Australia during summer. We show that models generally have a reduction in blocking frequency with future anthropogenic forcing, particularly in the Australia-New Zealand sector with the number of winter blocked days reduced by about one third by the end of the 21st century.

Plain Language Summary Atmospheric blocking is a process in which an atmospheric wave breaks, diverting the jet stream and any incoming storms to the north or south. A blocking event is characterized by high pressure on the poleward side and low pressure on the equatorward side and persists for upward of 4 days. A key feature of blocks is their persistence, which can lead to events, which have significant impacts on society including heat waves in summer and periods of extreme cold in winter. Climate models often do not simulate enough blocking events, though most research on this problem has focused on the Northern Hemisphere and less is known about the Southern Hemisphere. We survey 23 climate models and show that during winter some models simulate too many blocking events, while others simulate too few, whereas during summer, almost all models simulate too few events to the south of Australia. We also show that with higher concentrations of greenhouse gases we expect there to be less blocking, particularly to the south of Australia and over New Zealand during winter.

1. Introduction

Atmospheric blocking is an important aspect of the circulation in midlatitudes. It is characterized by a persistent reversal of the prevailing westerly flow and consequently the diversion of incoming weather systems to the north or south (Rex, 1950). The persistence of blocking events can have significant societal impacts as blocks are frequently linked with extreme weather (Gibson et al., 2017; Perkins-Kirkpatrick et al., 2016; Sillmann et al., 2011; Woollings et al., 2018). However, the simulation of atmospheric blocking has proved difficult as many general circulation models (GCMs) underestimate the frequency of events in key regions (D'Andrea et al., 1998; Woollings et al., 2018). If models fail to accurately capture blocking under present day conditions, then this reduces our confidence in their future projections of blocking frequency. Hence, it is important to document the biases inherent within GCMs and investigate how to alleviate them.

While model blocking biases and modeled future changes have been key areas of research in recent years, few papers have examined the Southern Hemisphere (SH). In this study, we document the SH blocking biases and future projections of a large set of GCMs taken from the Coupled Model Intercomparison Project Phase 5 (CMIP5; Taylor et al., 2012). We investigate whether, like in the Northern Hemisphere (NH), the models have a systematic bias in certain regions and how the models respond to a future scenario of anthropogenic forcing conditions.

In comparison to the NH, SH stationary waves are weaker (Nigam & DeWeaver, 2015; Trenberth & Mo, 1985), while zonal winds are stronger and transient phenomena like cyclones and blocking events are shorter lived (Berrisford et al., 2007). Midlatitude blocking in the SH primarily occurs over the South Pacific Ocean where the flow is relatively weak and is most frequent during southern winter (Berrisford et al., 2007; Renwick & Revell, 1999; Renwick, 2005; Sinclair, 1996; Trenberth & Mo, 1985). Blocking events have a notable effect on SH weather and have been shown to be associated with heat waves over New Zealand (Salinger et al., 2019) and Australia (Pezza et al., 2012; Perkins-Kirkpatrick et al., 2016; Risbey et al., 2018) and persistent frost events in Australia (Risbey et al., 2019) and South America (Müller & Berri, 2007). The occurrence of blocks also modulates precipitation over South America (Mendes et al., 2008; Rodrigues & Woollings, 2017) and Australia (Cowan et al., 2013; Grose et al., 2017; Pook et al., 2006, 2013; Tozer et al., 2018).

Most GCMs agree that the SH jet stream will strengthen and shift poleward in response to anthropogenic forcings (Barnes & Polvani, 2013; Simpson et al., 2014; Swart & Fyfe, 2012) changing the background flow on which transient events like blocking episodes occur. Several studies have shown that in response to these anthropogenic forcings, the number of cutoff lows decreases during all seasons (Dowdy et al., 2013; Grose et al., 2012). This is consistent with Matsueda et al. (2010), who found blocking frequency decreases in the Australia-New Zealand sector, though they found no change over the southeast Pacific. Similarly, Grose et al. (2017) examined blocking within the Australia region in 26 CMIP5 models and found blocking frequency to be reduced in future simulations. More broadly, a study by Parsons et al. (2016) using four GCMs from the CMIP5 ensemble showed that blocking frequency was reduced across most of the SH in future climate simulations, with some seasonal variations in the location of the largest changes.

This study adds to this literature by examining blocking over the entire SH in a wide range of models using techniques that have already been applied to NH blocking. The methods and data used are explained in section 2, while the biases and future projections are examined in section 3, and conclusions are given in section 4.

2. Data and Methods

2.1. Data

For this study we use daily mean geopotential height data on the 500-hPa level (Z500) from the 23 CMIP5 coupled models, which provided this field. From these models, we use the historical and Representative Concentration Pathway 8.5 experiments over the years 1979–2005 and 2070–2099, respectively. The former period is chosen to coincide with the beginning of the satellite era, as reanalysis data before this date are less reliable in the SH (Bromwich & Fogt, 2004). The full list of models examined is given in the supporting information. Daily mean ERA-Interim reanalysis data (ERAI; Dee et al., 2011) from the period 1979–2005 is taken to represent the observed state of the atmosphere. All fields are regridded onto a common N48 grid (1.875° × 1.875°) before blocking calculations are performed.

2.2. Methods

As discussed in Woollings et al. (2018), there exist many different indices with which to define blocking and these can broadly speaking be divided into two groups. The first of these defines a persistent anticyclone as the key feature of a block and the blocking index is constructed to look for persistent positive geopotential height or surface pressure anomalies (Parsons et al., 2016; Renwick & Revell, 1999). The second considers that a persistent reversal of the geopotential height or potential vorticity gradient better characterizes blocking (Davini et al., 2012; Tibaldi et al., 1994). We use an adaptation of the method of Masato et al. (2012). The original index from Masato et al. (2012) extended the method of Pelly and Hoskins (2003) to two dimensions. It used potential vorticity on the dynamical tropopause; however, Masato et al. (2013) showed that the use of geopotential height at 500 hPa, which is a readily available field in CMIP5 models, produced similar results.

In short, the algorithm calculates the difference in daily mean Z500 integrated over a line 11° to the north and 11° to the south of each grid point. For regions where the difference is negative and thus the usual meridional Z500 gradient is reversed, a "blocking center" is defined and tracked over the following days. If the blocking center continues to exist and remains sufficiently close to the original location, then this is defined as a blocking event. For a more complete description of the algorithm see Masato et al. (2013). In the original paper, Z500 was integrated poleward and equatorward of each grid point by 15° and not 11°; however, the frequency of SH blocking is considerably lower than in certain regions of the NH and so we choose 11° to improve the signal-to-noise ratio. Experiments comparing 11° with 15° show similar blocking

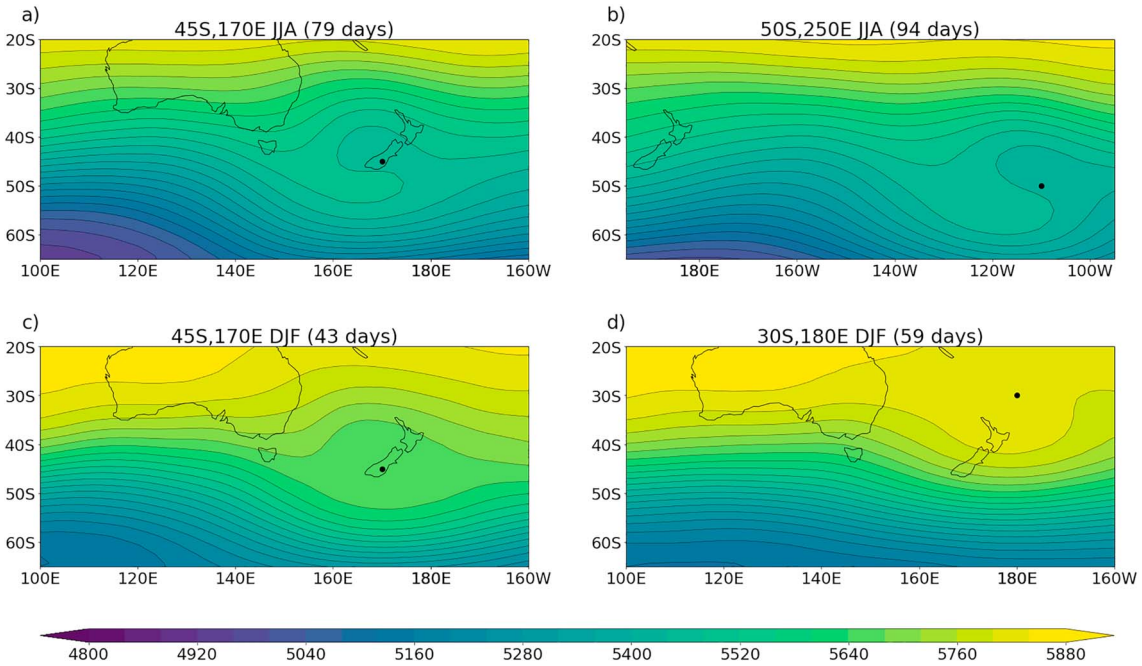

Figure 1. (a–d) Composites of daily mean Z500 for the onset day of blocking occurring at different locations. In each figure the location of the block is denoted by a black dot. The units are in meters. DJF = December–February; JJA = June–August.

frequency distributions, though the frequency is increased by about 30% (not shown). In accordance with Berrisford et al. (2007), we also set the threshold for persistence of the Z500 gradient reversal to 4 days rather than 5 days because of the typically lower persistence of SH blocks.

To ensure that the algorithm correctly identifies blocking events, we show composites of daily mean Z500 on the onset day of blocking events occurring at a few particular locations. Figures 1a and 1b show composites of blocking events during winter over New Zealand and in the southeast Pacific with a clear pattern of anticyclonic wave breaking. In both cases the events clearly disrupt the mean flow, justifying them being labeled as blocking. The same point over New Zealand during summer in Figure 1c does not show a clear overturning of contours but rather shows a poleward ridge and equatorward trough. Examination of individual events (not shown) indicates that detections by the algorithm normally do correspond to wave breaking, though they are split between anticyclonic and cyclonic wave breaking events, which may explain the smoothed-out composite. Finally, Figure 1d shows composites of events occurring at or near a point in the subtropics. Unlike the other cases, the main flow does not appear to be significantly altered by the block. There has been some debate about whether low-latitude events constitute blocking (Davini et al., 2012), though Rodrigues and Woollings (2017) showed that similar events over South America can have important impacts on local weather. Similarly, the index detects a high frequency of blocking events at high latitudes, in agreement with other authors (Berrisford et al., 2007; Masato et al., 2013). These events are often called "high-latitude blocking" or simply "wave breaking" (Berrisford et al., 2007; Woollings et al., 2008), and again, we do not refer to these as blocking because they are located poleward of the main band of westerlies and so do not tend to "block" the main flow. In this paper we take the approach of focusing on events in midlatitudes as these cohere more strongly with the traditional view of blocking.

3. Results

3.1. Background Flow

Before investigating blocking frequencies in the SH, we show zonal wind on the 300-hPa level to understand the historical biases and future changes in the time-mean background flow, as the configuration of the background flow influences the likelihood of blocking events.

As shown in Figure 2b, the summer circulation is relatively zonally symmetric and strong at all longitudes, whereas during winter (Figure 2a) there are distinct zonal asymmetries with the split jet (Bals-Elsholz et al., 2001; Inatsu & Hoskins, 2006) dominating over the South Pacific. The midlatitude flow is weaker over the

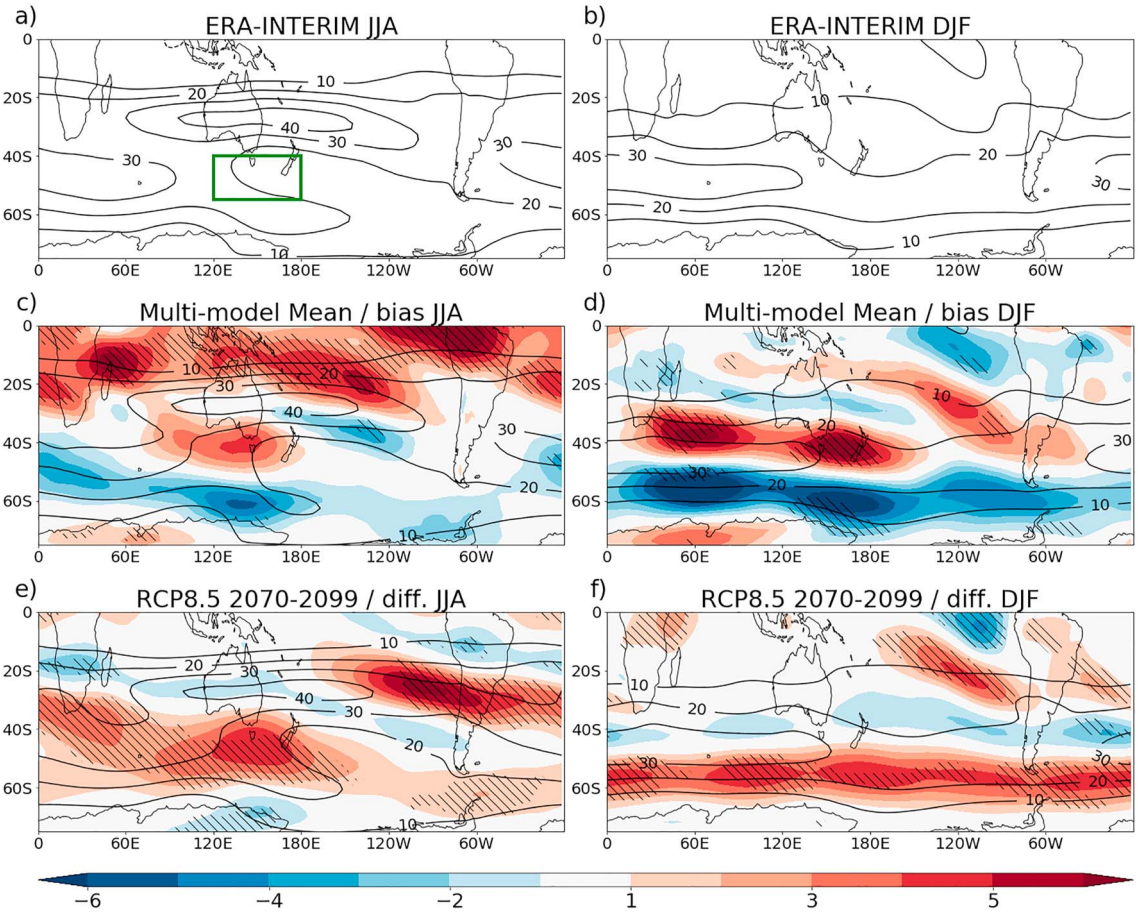

Figure 2. The 300-hPa zonal wind biases and future projections in the Southern Hemisphere for winter (JJA, left) and summer (DJF, right): (a, b) Climatology in ERAI reanalysis for the period 1979–2005; (c, d) the multimodel mean climatology over the same period in the historical simulations (contours) and multimodel mean minus ERAI (colors); (e, f) multimodel mean climatology for the period 2070–2099 in the RCP 8.5 scenario (contours) and future projections minus historical simulations (colors). Hatching indicates that 80% of models agree on the sign of the difference. The green box in (a) indicates the Australia-New Zealand region referred to later on. The units are in meters per second. ERAI = ERA-Interim; DJF = December–February; JJA = June–August; RCP 8.5 = Representative Concentration Pathway 8.5.

South Pacific during winter, enhancing the likelihood of wave breaking and the development of a blocking event (Nakamura & Huang, 2018).

The equatorward zonal mean jet bias in CMIP5 has been well documented (Bracegirdle et al., 2013; Son et al., 2010; Swart & Fyfe, 2012; Wilcox et al., 2012) and has been linked to an overly persistent Southern Annular Mode (Kidston & Gerber, 2010), shortwave cloud forcing biases (Ceppi et al., 2012), and underestimated low level orographic drag (Pithan et al., 2016). Figures 2c and 2d indicate that there are zonal asymmetries to the historical jet bias, especially during winter as the bias is concentrated to the south of Australia, contributing to an overly weak split jet structure. The hatching indicates that there is greater intermodel agreement on the sign of the bias during December–February than June–August.

Almost all CMIP5 models feature a poleward jet shift and strengthening in response to anthropogenic forcing (Barnes & Polvani, 2013; Swart & Fyfe, 2012), and these strengthened westerly winds may reduce the probability of blocking events in future. Similar to the historical jet bias, Figure 2e shows that though there are overall increases in wind speed across the midlatitudes, there are clear zonal asymmetries in the winter response. The region south of Australia shows the greatest increase in upper tropospheric wind in the SH midlatitudes with a mean increase of up to 4–5 m/s and strong agreement between the different models on the sign of the change.

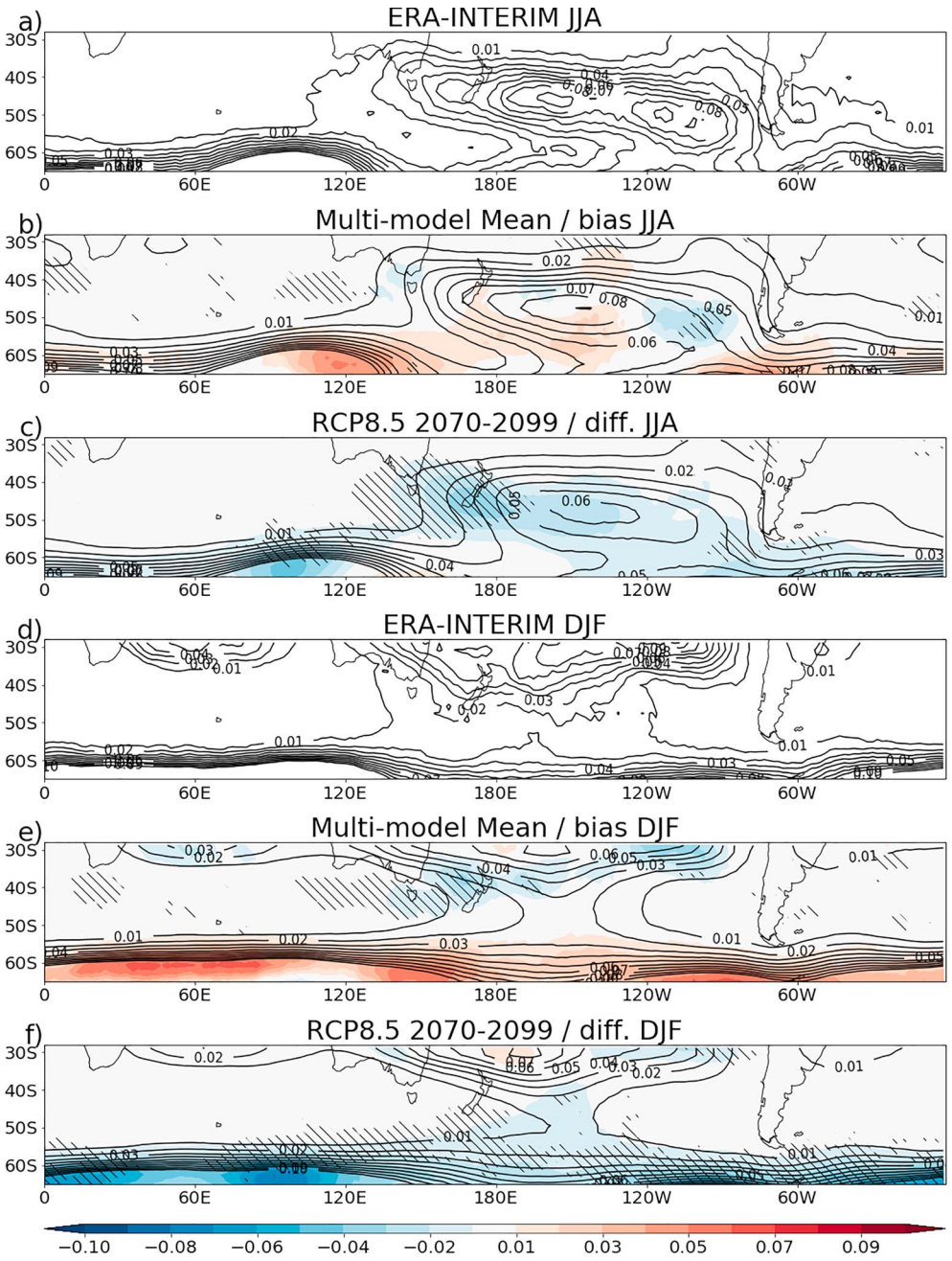

Figure 3. Blocking frequency biases and future projections in the Southern Hemisphere for winter (a–c) and summer (d–f): (a, d) The ERAI mean blocking frequency for each gridpoint; (b, e) the mean of all CMIP5 models for the historical experiment (contours) minus ERAI (colors); (c, f) the mean of all CMIP5 models for the RCP 8.5 scenario from 2070–2099 (contours) minus the historical experiment (colors). The contour interval for all plots is 0.01, and hatching indicates that 80% of models agree on the sign of the difference. The blocking frequency is given as the fraction of blocked days. CMIP5 = Coupled Model Intercomparison Project Phase 5; JJA = June–August; ERAI = ERA-Interim; DJF = December–February.

3.2. Blocking Biases

We now examine the biases in blocking frequency of the CMIP5 models from the observed climatology taken from reanalysis. Figure 3 shows the blocking frequency calculated from ERAI data and from historical and future simulations. In agreement with the literature, blocking occurs most frequently during winter (Figure 3a) and predominantly over the South Pacific Ocean (Berrisford et al., 2007; Parsons et al., 2016; Renwick, 2005; Sinclair, 1996; Trenberth & Mo, 1985). The winter blocking frequency maximum, east of

New Zealand, is shifted slightly equatorward with respect to studies such as Renwick (2005), which use persistent positive anomaly methods as these locate blocking events at the anticyclonic anomaly rather than at the location of the Z500 reversal. In addition, there is no local maximum southeast of South America as in Trenberth and Mo (1985) and Renwick (2005). Figure 3a shows a slight double maximum, which is also seen in Sinclair (1996) and Renwick (2005), though is not prominent in other studies and may be an artifact of the short sampling period.

The first thing to notice about the winter CMIP5 blocking bias in Figure 3b is the lack of hatching, indicating that models do not exhibit a consistent bias during this season. Examination of the individual models, which can be found in the supporting information, indicates that models often do have significant biases but that when taking the multimodel mean, these biases largely cancel one another out. The lowest-resolution models (bcc-csm1-1-m, BNU-ESM, CanESM2, CMCC-CESM, and ISPL-CM5A-LR) all underestimate blocking frequency on the equatorward side of the polar-front jet indicating that there may be a minimum resolution necessary to successfully simulate blocking; however, there is not necessarily a monotonic improvement with resolution as some high-resolution models also show considerable blocking underestimation (e.g., CCSM4).

Observed summer blocking frequency (Figure 3d) is lower than during winter, with the region of blocking located further west, over the western and central South Pacific. The CMIP5 ensemble places the blocking frequency maximum slightly eastward of ERAI, and most models underestimate summer blocking to the south and southeast of Australia. This is likely related to the positive wind bias in this region (Figure 2), which in turn is related to the overly equatorward jets in CMIP5.

3.3. Blocking Future Projections

In terms of future projections, Figures 3c and 3f indicate that blocking frequency in the CMIP5 ensemble-mean generally decreases with anthropogenic forcing during winter and summer. Previous work (Matsueda et al., 2010; Parsons et al., 2016) has shown this to be the case in a small subset of models, but using a larger ensemble allows us to rule out the influence of natural variability, which is considerable for blocking frequency, and to show that the result is robust to model choice. In particular, there is strong intermodel agreement on reduced high-latitude blocking in summer, which is consistent with the strengthening of high-latitude winds (Figures 2e and 2f) and on blocking reductions south of Australia and over New Zealand during winter. The latter result is in agreement with Parsons et al. (2016), who used a persistent positive pressure anomaly method and found the largest winter changes in that region (see their Figure 6b) and with Grose et al. (2017). This result is also coherent with the reductions in cutoff low events found by Grose et al. (2012) and Dowdy et al. (2013). Reductions in overall blocking frequency may be the result of a decrease in the number of blocking events or a reduction in the mean duration of blocking events. A decomposition of this, which can be found in the supporting information, shows that both effects play a role; however changes in the number of events seem to be more significant. We now turn to examining the Australia-New Zealand region in more detail.

3.4. Winter Blocking Frequency Decreases in the Australia-New Zealand Sector

The largest anthropogenically forced changes to the winter midlatitude circulation in the SH occur to the south of Australia (Figure 2), coincident with blocking frequency decreases seen in Figure 3. To investigate this further, we define the region between 120–180°E and 40–55°S (shown by the green box in Figure 2a) to be the Australia-New Zealand region (AusNZ) and count the number of blocked days, which occur within this area each season. For a day to be defined as "blocked" there must be at least one blocked gridpoint within this region.

In Figure 4a, we plot the mean number of blocked days per winter season for the Representative Concentration Pathway 8.5 scenario in the period 2070–2099 against the historical period. Significantly, all ensemble members but one show a decrease in blocking frequency as they all lie below the blue dashed line (the exception being EC-Earth r2i1p1, which remains virtually the same). This is all the more remarkable given the spread of historical blocking frequency among CMIP5. Blocking frequency varies substantially from year to year and so sampling uncertainty may play a role. In order to quantify this, we plot the 95% confidence intervals on the ERAI value, calculated by resampling the number of blocking days for each year with replacement 1,000 times, calculating the mean each time and taking the confidence intervals as the 2.5th and 97.5th percentiles. Interestingly, the multimodel mean historical blocking lies close to the ERAI mean and within the confidence intervals, even though upper tropospheric wind speed is generally significantly

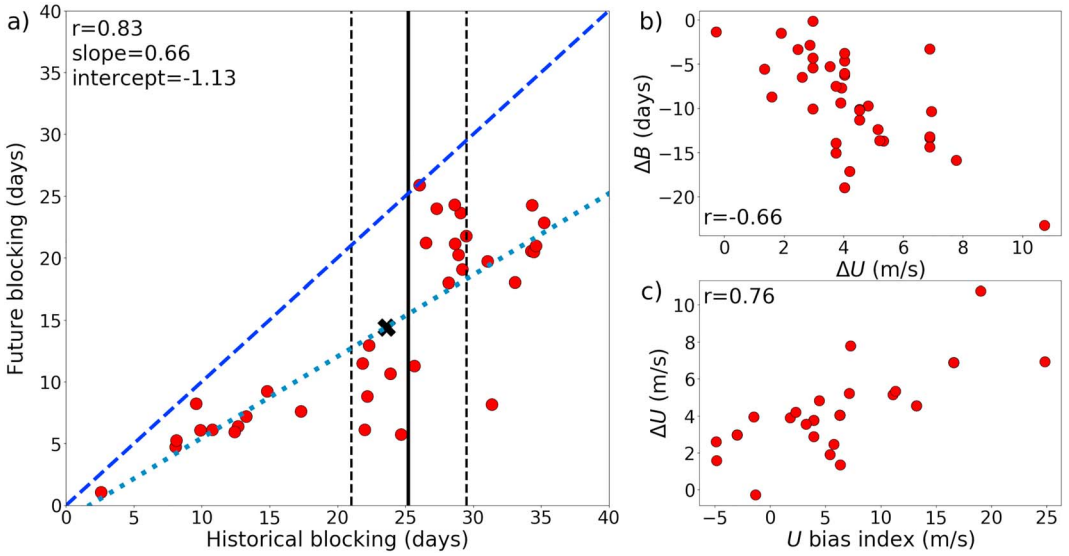

Figure 4. Changes in the number of blocked days per season in the Australia-New Zealand region (AusNZ) during winter: (a) Mean blocking days per season for future and historical simulations for all ensemble members. The cross represents the multimodel mean, the dashed line is the line with the *y* value equal to the corresponding *x* value, the dotted line is the line of best fit, the solid black line is the ERA-Interim mean, while the dashed vertical lines are the 95% confidence intervals (see text for details). (b) Blocking days per season change against the change in 300-hPa zonal wind. (c) The change in 300-hPa zonal wind against the zonal wind bias index (see text for details).

overestimated in this region in models (Figure 2c). This is in contrast to central Europe where a positive wind bias results in strongly underestimated blocking (Scaife et al., 2010).

In general, the blocking frequency in a future simulation decreases by about a third in comparison to the corresponding historical simulation, exceeding the internal variability in mean blocking days between ensemble members of the same model (supporting information). However, there is a considerable spread in future blocking frequency and even for the historical simulations, which lie close to the ERAI value (black line), the spread in future projections is large at between 5 and 25 days per season. Blocking frequency changes are likely to be driven by changes to the large-scale circulation (de Vries et al., 2013; Woollings, 2010). To investigate if this is the case, the relationship between blocking changes in the AusNZ region and changes in mean zonal wind for each model is shown in Figure 4b. From this, it is clear that larger wind increases result in larger reductions in blocking frequency with the wind change accounting for about 44% of the intermodel variance in blocking change.

In addition, several authors have noted a relationship between the zonal mean historical jet latitude and the magnitude of the future poleward jet shift/jet strengthening (Barnes & Polvani, 2013; Bracegirdle et al., 2013; Kidston & Gerber, 2010; Simpson & Polvani, 2016) suggesting that there is a relationship between the historical winds and the wind change. Figure 2 indicates that there is both a strong wind bias and a strong response within the AusNZ sector, and as the blocking change is linked to the wind response, it may be that the wind bias seen in Figure 2 influences this. To quantify the strength, locally, of the relationship between the zonal wind response and the historical wind bias, we construct a wind bias index. This is defined as the difference between the winter mean zonal wind at 300 hPa over the latitudes 35–45°S and 55–65°S, both between 120°E and 180°E, minus the same index in ERAI. Figure 4c shows that the zonal wind response in the AusNZ region is strongly related to the historical wind bias as models with a strong bias index show an enhanced response. While it is apparent that all models show an increase in wind speed, considering the bias-response relationship, the true wind response may lie closer to 2–3 m/s than the 4–5 m/s seen in Figure 2e, and hence, the change in blocking days per winter season is unlikely to be more than 10 days (Figure 4b). These results also seem to be coherent with Grose et al. (2017), who found that models with a more positive blocking bias, tended to show a greater reduction in winter blocking days.

4. Discussion and Conclusions

In this study we have examined SH blocking in 23 coupled models from CMIP5 and investigated biases in blocking frequency and how mean blocking frequency is altered under conditions of increased greenhouse gas forcing. We have shown that models do not exhibit blocking biases of the same sign during winter, though the biases themselves may be large, while models consistently have too little blocking to the south of Australia during summer. The latter finding is likely related to the overly equatorward jets found in most of the current generation of models during summer, whereas jet biases are less consistently of the same sign in winter.

In recent years considerable attention has been given to the fact that models systematically underestimate blocking over Europe (Masato et al., 2013). Examining model blocking in the SH using many of the same models that have been shown to underestimate blocking over Europe has indicated that these biases are likely to be highly region-dependent and blocking underestimation is not necessarily a global property of the CMIP5 models. This result is in agreement with Parsons et al. (2016), who found differing blocking biases between the four CMIP5 models in their study.

In terms of future projections, the most significant changes to summer blocking occur primarily at high latitudes, well away from regions, such as Australia, which are affected by heat waves (Figure 3f). However, this does not imply that the frequency and severity of heat waves will not change. First, it is likely that the driving force behind the increased occurrence of heat waves (Perkins-Kirkpatrick et al., 2016) is thermodynamic rather than dynamic in origin. Second, the Masato et al. (2013) index only captures large-scale events, and it may be that smaller wave breaking events are important for heat waves. For example, heat waves over southeast Australia are often associated with wave breaking in which a large anticyclonic air mass is encircled by a relatively thin filament of cyclonic air (Parker et al., 2014).

In winter we found a general reduction in SH blocking frequency as in Parsons et al. (2016). In particular, we noted that there is strong model agreement on decreases to the south of Australia and over New Zealand during austral winter, corroborating the results of Grose et al. (2017). This could have significant implications for rainfall in this region as blocking is often associated with cutoff cyclones over southeast Australia (Pook et al., 2006) and for the occurrence of frost events (Risbey et al., 2019). However, further work would be required to quantify these changes. The blocking frequency reductions over the southeast Pacific show less model agreement, and thus, changes to blocking-related weather over South America are less certain.

The local changes in blocking to the south of Australia appear to be linked to large-scale changes in the winter atmospheric circulation (Figure 4b) as this region experiences a particularly strong zonal wind increase. This is associated with a reduction in the extent of the climatological split in the flow (Figure 2). This then raises the question of what mechanisms are driving the large-scale winter circulation changes in models. Is this a result of local or remote forcing? Answering these questions is beyond the scope of this current article, but we provide some brief speculations. It is possible that the alteration of the climatological stationary Rossby wave, which contributes to the split jet structure (Inatsu & Hoskins, 2006), could result in the changes seen in CMIP5. Freitas and Rao (2014) showed that this stationary Rossby wave tends to weaken with anthropogenic forcing in CMIP3 models. These changes could result from tropical forcing via altered Rossby wave generation or in midlatitudes through alteration of the background state. Model experiments could be employed to answer this question more fully.

Acknowledgments
We would like to thank two anonymous reviewers for their constructive comments which helped to improve the manuscript. We acknowledge ECMWF for the ERA-INTERIM data set and the World Climate Research Programme's Working Group on Coupled Modelling, which is responsible for CMIP. We thank the climate modeling groups (listed in the supporting information) for producing and making available their model output. The ERA-INTERIM data for the work in this paper were downloaded from the ECMWF website (https://www.ecmwf.int/en/forecasts/datasets/browse-reanalysis-datasets), while CMIP5 data were obtained from the BADC archive on the CEDA data server (available here http://data.ceda.ac.uk/badc/). We would also like to thank Marie Drouard for helpful discussions on the blocking code. Matthew Patterson was funded by the Natural Environment Research Council (Grant NE/L002612/1).

References

Bals-Elsholz, T. M., Atallah, E. H., Bosart, L. F., Wasula, T. A., Cempa, M. J., & Lupo, A. R. (2001). The wintertime Southern Hemisphere split jet: Structure, variability, and evolution. *Journal of Climate*, *14*(21), 4191–4215. https://doi.org/10.1175/1520-0442(2001)014h4191:TWSHSJi2.0.CO;2

Barnes, E. A., & Polvani, L. (2013). Response of the midlatitude jets, and of their variability, to increased greenhouse gases in the CMIP5 models. *Journal of Climate*, *26*(18), 7117–7135. https://doi.org/10.1175/JCLI-D-12-00536.1

Berrisford, P., Hoskins, BJ, & Tyrlis, E. (2007). Blocking and Rossby wave breaking on the dynamical tropopause in the Southern Hemisphere. *Journal of the Atmospheric Sciences*, *64*, 2881–2898. https://doi.org/10.1175/JAS3984.1

Bracegirdle, T. J., Shuckburgh, E., Sallee, J. B., Wang, Z., Meijers, A. J. S., Bruneau, N., et al. (2013). Assessment of surface winds over the atlantic, indian, and pacific ocean sectors of the Southern Ocean in CMIP5 models: Historical bias, forcing response, and state dependence. *Journal of Geophysical Research: Atmospheres*, *118*, 547–562. https://doi.org/10.1002/jgrd.50153

Bromwich, D. H., & Fogt, R. L. (2004). Strong trends in the skill of the ERA-40 and NCEP-NCAR reanalyses in the high and midlatitudes of the Southern Hemisphere, 1958–2001*. *Journal of Climate*, *17*(23), 4603–4619. https://doi.org/10.1175/3241.1

Ceppi, P., Hwang, Y. T., Frierson, D. M. W., & Hartmann, D. L. (2012). Southern Hemisphere jet latitude biases in CMIP5 models linked to shortwave cloud forcing. *Geophysical Research Letters*, *39*, L19708. https://doi.org/10.1029/2012GL053115

Cowan, T., van Rensch, P., Purich, A., & Cai, W. (2013). The association of tropical and extratropical climate modes to atmospheric blocking across southeastern Australia. *Journal of Climate*, *26*(19), 7555–7569. https://doi.org/10.1175/JCLI-D-12-00781.1

D'Andrea, F., Tibaldi, S., Blackburn, M., Boer, G., Déqué, M., Dix, M. R., et al. (1998). Northern Hemisphere atmospheric blocking as simulated by 15 atmospheric general circulation models in the period 1979–1988. *Climate Dynamics*, *14*(6), 385–407. https://doi.org/10.1007/s003820050230

Davini, P., Cagnazzo, C., Gualdi, S., & Navarra, A. (2012). Bidimensional diagnostics, variability, and trends of Northern Hemisphere blocking. *Journal of Climate*, *25*(19), 6496–6509. https://doi.org/10.1175/JCLI-D-12-00032.1

de Vries, H., Woollings, T., Anstey, J., Haarsma, R. J., & Hazeleger, W. (2013). Atmospheric blocking and its relation to jet changes in a future climate. *Climate Dynamics*, *41*(9–10), 2643–2654. https://doi.org/10.1007/s00382-013-1699-7

Dee, D. P., Uppala, S. M., Simmons, A. J., Berrisford, P. , Poli, P. , Kobayashi, S. , Andrae, U. , Balmaseda, M. A., Balsamo, G. , Bauer, P. , Bechtold, P. , Beljaars, A. C., van de Berg, L. , Bidlot, J. , Bormann, N. , Delsol, C. , Dragani, R. , Fuentes, M. , Geer, A. J., Haimberger, L. , Healy, S. B., Hersbach, H. , Hólm, E. V., Isaksen, L. , Kållberg, P. , Köhler, M. , Matricardi, M. , McNally, A. P., Monge-Sanz, B. M., Morcrette, J. , Park, B. , Peubey, C. , de Rosnay, P. , Tavolato, C. , Thépaut, J., & Vitart, F. (2011). The ERA-Interim reanalysis: configuration and performance of the data assimilation system. *Quarterly Journal of the Royal Meteorological Society*, *137*, 553–597. https://doi.org/10.1002/qj.828

Dowdy, A. J., Mills, G. A., Timbal, B., & Wang, Y. (2013). Changes in the risk of extratropical cyclones in eastern Australia. *Journal of Climate*, *26*(4), 1403–1417. https://doi.org/10.1175/JCLI-D-12-00192.1

Freitas, A. C. V., & Rao, V. Brahmananda (2014). Global changes in propagation of stationary waves in a warming scenario. *Quarterly Journal of the Royal Meteorological Society*, *140*(679), 364–383. https://doi.org/10.1002/qj.2151

Gibson, P. B., Pitman, A. J., Lorenz, R., & Perkins-Kirkpatrick, S. E. (2017). The role of circulation and land surface conditions in current and future Australian heat waves. *Journal of Climate*, *30*(24), 9933–9948. https://doi.org/10.1175/JCLI-D-17-0265.1

Grose, M. R., Pook, M. J., McIntosh, P. C., Risbey, J. S., & Bindoff, N. L. (2012). The simulation of cutoff lows in a regional climate model: Reliability and future trends. *Climate Dynamics*, *39*(1–2), 445–459. https://doi.org/10.1007/s00382-012-1368-2

Grose, M. R., Risbey, J. S., Moise, A. F., Osbrough, S., Heady, C., Wilson, L., & Erwin, T. (2017). Constraints on southern Australian rainfall change based on atmospheric circulation in CMIP5 simulations. *Journal of Climate*, *30*(1), 225–242. https://doi.org/10.1175/JCLI-D-16-0142.1

Inatsu, M., & Hoskins, B. J. (2006). The seasonal and wintertime interannual variability of the split jet and the storm-track activity minimum near New Zealand. *Journal of the Meteorological Society of Japan*, *84*(3), 433–445.

Kidston, J., & Gerber, E. P. (2010). Intermodel variability of the poleward shift of the austral jet stream in the CMIP3 integrations linked to biases in 20th century climatology. *Geophysical Research Letters*, *37*, L09708. https://doi.org/10.1029/2010GL042873

Müller, G. V., & Berri, G. J. (2007). Atmospheric circulation associated with persistent generalized frosts in central-southern South America. *Monthly Weather Review*, *135*(4), 1268–1289. https://doi.org/10.1175/MWR3344.1

Masato, G., Hoskins, B. J., & Woollings, T. J. (2012). Wave-breaking characteristics of midlatitude blocking. *Quarterly Journal of the Royal Meteorological Society*, *138*(666), 1285–1296. https://doi.org/10.1002/qj.990

Masato, G., Hoskins, B. J., & Woollings, T. (2013). Wave-breaking characteristics of Northern Hemisphere winter blocking: A two-dimensional approach. *Journal of Climate*, *26*(13), 4535–4549. https://doi.org/10.1175/JCLI-D-12-00240.1

Matsueda, M., Endo, H., & Mizuta, R. (2010). Future change in Southern Hemisphere summertime and wintertime atmospheric blockings simulated using a 20-km-mesh AGCM. *Geophysical Research Letters*, *37*, L02803. https://doi.org/10.1029/2009GL041758

Mendes, M. C. D., Trigo, R. M., Cavalcanti, I. F. A. A. A., & DaCamara, C. C. (2008). Blocking episodes in the Southern Hemisphere: Impact on the climate of adjacent continental areas. *Pure and Applied Geophysics*, *165*, 1941–1962. https://doi.org/10.1007/s00024-008-0409-4

Nakamura, N., & Huang, ClareSY (2018). Atmospheric blocking as a traffic jam in the jet stream. *Science (New York, N.Y.)*, *361*(6397), 42–47. https://doi.org/10.1126/science.aat0721

Nigam, S., & DeWeaver, E. (2015). Dynamical meteorology | stationary waves (orographic and thermally forced). *Encyclopedia of Atmospheric Sciences*, *2*, 431–445. https://doi.org/10.1016/B978-0-12-382225-3.00381-9

Parker, T. J., Berry, G. J., & Reeder, M. J. (2014). The structure and evolution of heat waves in Southeastern Australia. *Journal of Climate*, *27*, 5768–5785. https://doi.org/10.1175/JCLI-D-13-00740.1

Parsons, S., Renwick, J. A., & McDonald, A. J. (2016). An assessment of future Southern Hemisphere blocking using CMIP5 projections from four GCMs. *Journal of Climate*, *29*(21), 7599–7611. https://doi.org/10.1175/JCLI-D-15-0754.1

Pelly, J. L., & Hoskins, B. J. (2003). A new perspective on blocking. *Journal of the Atmospheric Sciences*, *60*, 743–755.

Perkins-Kirkpatrick, S. E., White, C. J., Alexander, L. V., Argüeso, D., Boschat, G., Cowan, T., et al. (2016). Natural hazards in Australia: Heatwaves. *Climatic Change*, *139*(1), 101–114. https://doi.org/10.1007/s10584-016-1650-0

Pezza, A. B., van Rensch, P., & Cai, W. (2012). Severe heat waves in Southern Australia: Synoptic climatology and large scale connections. *Climate Dynamics*, *38*(1-2), 209–224. https://doi.org/10.1007/s00382-011-1016-2

Pithan, F., Shepherd, T. G., Zappa, G., & Sandu, I. (2016). Climate model biases in jet streams, blocking and storm tracks resulting from missing orographic drag. *Geophysical Research Letters*, *43*, 7231–7240. https://doi.org/10.1002/2016GL069551

Pook, M. J., McIntosh, P. C., & Meyers, G. A. (2006). The synoptic decomposition of cool-season rainfall in the southeastern Australian cropping region. *Journal of Applied Meteorology and Climatology*, *45*(8), 1156–1170. https://doi.org/10.1175/JAM2394.1

Pook, M. J., Risbey, J. S., Mcintosh, P. C., Ummenhofer, C. C., Marshall, A. G., & Meyers, G. A. (2013). The seasonal cycle of blocking and associated physical mechanisms in the Australian region and relationship with rainfall. *Monthly Weather Review*, *141*, 4534–4553. https://doi.org/10.1175/MWR-D-13-00040.1

Renwick, J. A. (2005). Persistent positive anomalies in the Southern Hemisphere circulation. *Monthly Weather Review*, *133*(4), 977–988. https://doi.org/10.1175/MWR2900.1

Renwick, J. A., & Revell, M. J. (1999). Blocking over the South Pacific and Rossby wave propagation. *Monthly Weather Review*, *127*, 4160–4161.

Rex, D. F. (1950). Blocking action in the middle troposphere and its effect upon regional climate. *Tellus*, *2*(3), 196–211. https://doi.org/10.1111/j.2153-3490.1950.tb00331.x

Risbey, J. S., Monselesan, D. P., O'Kane, T. J., Tozer, C. R., Pook, M. J., & Hayman, P. T. (2019). Synoptic and large-scale determinants of extreme austral frost events. *Journal of Applied Meteorology and Climatology*, *58*(5), 1103–1124. https://doi.org/10.1175/JAMC-D-18-0141.1

Risbey, J. S., O'Kane, T. J., Monselesan, D. P., Franzke, ChristianL. E., & Horenko, I. (2018). On the dynamics of austral heat waves. *Journal of Geophysical Research: Atmospheres*, *123*, 38–57. https://doi.org/10.1002/2017JD027222

Rodrigues, R., & Woollings, T. (2017). Impact of atmospheric blocking on South America in austral summer. *Journal of Climate*, *30*, 1821–1837.

Salinger, M. J., Renwick, J., Behrens, E., Mullan, ABrett, Diamond, H. J., Sirguey, P., et al. (2019). The unprecedented coupled ocean-atmosphere summer heatwave in the New Zealand region 2017/18: Drivers, mechanisms and impacts. *Environmental Research Letters*, *14*(4), 44023. https://doi.org/10.1088/1748-9326/ab012a

Scaife, A. A., Woollings, T., Knight, J., Martin, G., & Hinton, T. (2010). Atmospheric blocking and mean biases in climate models. *Journal of Climate*, *23*(23), 6143–6152. https://doi.org/10.1175/2010JCLI3728.1

Sillmann, J., Croci-Maspoli, M., Kallache, M., Katz, R. W., Sillmann, J., Croci-Maspoli, M., et al. (2011). Extreme cold winter temperatures in Europe under the influence of North Atlantic atmospheric blocking. *Journal of Climate*, *24*(22), 5899–5913. https://doi.org/10.1175/2011JCLI4075.1

Simpson, I. R., & Polvani, L. M. (2016). Revisiting the relationship between jet position, forced response, and annular mode variability in the southern midlatitudes. *Geophysical Research Letters*, *43*, 2896–2903. https://doi.org/10.1002/2016GL067989

Simpson, I. R., Shaw, T., & Seager, R. (2014). A diagnosis of the seasonally and longitudinally varying mid-latitude circulation response to global warming. *Journal of the Atmospheric Sciences*, *71*, 2489–2515. https://doi.org/10.1175/JAS-D-13-0325.1

Sinclair, M. R. (1996). A climatology of anticyclones and blocking for the Southern Hemisphere. *Monthly Weather Review*, *124*(2), 245–264. https://doi.org/10.1175/1520-0493(1996)124h0245:ACOAABi2.0.CO;2

Son, S.-W., Gerber, E. P., Perlwitz, J., Polvani, L. M., Gillett, N. P., Seo, K.-H., et al. (2010). Impact of stratospheric ozone on Southern Hemisphere circulation change: A multimodel assessment. *Journal of Geophysical Research*, *115*, D00M07. https://doi.org/10.1029/2010JD014271

Swart, N. C., & Fyfe, J. C. (2012). Observed and simulated changes in the Southern Hemisphere surface westerly wind-stress. *Geophysical Research Letters*, *39*, L16711. https://doi.org/10.1029/2012GL052810

Taylor, K. E., Stouffer, R. J., & Meehl, G. A. (2012). An overview of CMIP5 and the experiment design. *Bulletin of the American Meteorological Society*, *93*(4), 485–498. https://doi.org/10.1175/BAMS-D-11-00094.1

Tibaldi, S., Tosi, E., Navarra, A., & Pedulli, L. (1994). Northern and Southern Hemisphere seasonal variability of blocking frequency and predictability. *Monthly Weather Review*, *122*(9), 1971–2003. https://doi.org/10.1175/1520-0493(1994)122h1971:NASHSVi2.0.CO;2

Tozer, C. R., Risbey, J. S., O'Kane, T. J., Monselesan, D. P., & Pook, M. J. (2018). The relationship between wave trains in the Southern Hemisphere storm track and rainfall extremes over Tasmania. *Monthly Weather Review*, *146*(12), 4201–4230. https://doi.org/10.1175/MWR-D-18-0135.1

Trenberth, K. F., & Mo, K. C. (1985). Blocking in the Southern Hemisphere. *Monthly Weather Review*, *113*(1), 3–21. https://doi.org/10.1175/1520-0493(1985)113h0003:BITSHi2.0.CO;2

Wilcox, L. J., Charlton-Perez, A. J., & Gray, L. J. (2012). Trends in austral jet position in ensembles of high- and low-top CMIP5 models. *Journal of Geophysical Research*, *117*, D13115. https://doi.org/10.1029/2012JD017597

Woollings, T. (2010). Dynamical influences on European climate: An uncertain future. *Philosophical transactions. Series A, Mathematical, physical, and engineering sciences*, *368*(1924), 3733–3756. https://doi.org/10.1098/rsta.2010.0040

Woollings, T., Barriopedro, D., Methven, J., Son, S.-W., Martius, O., Harvey, B., et al. (2018). Blocking and its response to climate change. *Current Climate Change Reports*, *4*, 287–300. https://doi.org/10.1007/s40641-018-0108-z

Woollings, T., Hoskins, B., Blackburn, M., & Berrisford, P. (2008). A new Rossby wave-breaking interpretation of the North Atlantic oscillation. *Journal of the Atmospheric Sciences*, *65*, 609–626. https://doi.org/10.1175/2007JAS2347.1